

DESY SR-78/23
December 1978

DESY-Bibliothek

31. JAN. 1979

RESONANT PHOTOEMISSION FROM SmS(100)

by

W. Gudat, S. F. Alvarado and M. Campagna

Institut für Festkörperforschung der Kernforschungsanlage Jülich GmbH

To be sure that your preprints are promptly included in the
HIGH ENERGY PHYSICS INDEX ,
send them to the following address (if possible by air mail) :

DESY
Bibliothek
Notkestrasse 85
2 Hamburg 52
Germany

Resonant Photoemission from SmS(100)

W. Gudat, S.F. Alvarado and M. Campagna

Institut für Festkörperforschung der Kernforschungs-
anlage Jülich GmbH, Postfach 1913, D-5170 Jülich

Abstract

A strong, sharp resonance enhancement of 4f photoemission has been observed on SmS(100) surfaces for photon energies in the region of the 4d-4f transitions at about 126 eV. The discrete final state reached via the excitation $h\nu + 4d^{10}4f^6 \rightarrow 4d^9 4f^7$ autoionizes primarily via a super Coster-Kronig transition of the type $4d^9 4f^7 \rightarrow 4d^{10} 4f^5 + \text{unbound electron}$. Other decay channels, e.g. Sm 5p emission, as well as a surface induced binding energy shift in the Sm^{3+} final state are identified and discussed.

Solid State Communications

Basic features of the 4f photoemission spectra of rare earth metals and compounds have been recently clarified using monochromatized Al-K α radiation (XPS). They include: (1) relative position and (2) relative intensities of the 4f multiplets. (3) absolute position (i.e. binding energies) of the 4f states with respect to a fixed reference level (usually the Fermi level)¹.

Tunable synchrotron radiation has not been used so far in 4f photoemission studies of well-characterized surfaces of 4f materials in the region of the 4d-4f resonance absorption, occurring at energies between 105 eV (Ce) and 175 eV (Tm). We report here on the observation in this photon energy region of a large and sharp resonance enhancement of the 4f photoemission, which we have detected in a number of rare earth compounds and which we interpret, in analogy to recent work on Ni(100)², as a result of a Fano-type resonance. In addition, earlier discrepancies³ between the predicted and observed X-ray photoemission spectra of the Sm 4f levels in the semiconducting, black phase of SmS are resolved and evidence for the existence of a "surface induced binding energy shift" on SmS(100) is presented. We also briefly discuss the spectrum of the Sm 5p core levels and the importance of other decay mechanisms for the Sm excited state $4d^9 4f^7$. We present here data obtained on SmS only, although analogous observations (resonance effects) have also been made on other rare earth compounds. The conclusions reached here regarding the resonant photoemission are therefore expected to be valid for all the rare earth materials with incomplete 4f shell.

The experiments were performed at the storage ring DORIS in Hamburg using photon energies $h\nu$ in the region $15 < h\nu < 160$ eV from the "Flipper"-monochromator⁴. Spectra were recorded using a commercial double pass cylindrical mirror analyzer. For the energy distribution curves (EDC) the over-

all energy resolution is 0.4 to 0.45 eV at 120 eV, while for the constant final state spectra (CFS) the resolution is < 0.3 eV. Single crystals of SmS were cleaved in situ and measured at a base pressure of 3×10^{-10} Torr. Further experimental details will be reported elsewhere⁵.

In Fig. 1 we present energy distribution curves of SmS in the photon energy range $116.3 < h\nu < 129.2$ eV. For comparison we also show in the upper part an earlier XPS spectrum taken at $h\nu = 1486$ eV¹. At $h\nu = 116.3$ eV the Sm 4f photoemission cross section is already much larger than the one of the S(3p) valence states⁶, which are known to be located in the binding energy region between 3 and 8 eV below E_F ⁷. The observed intensity in Fig. 1 can therefore primarily be ascribed to 4f photoemission. All the EDC's have been normalized to the intensity (area) of the first leading peak, we label I_1 and which is known, at soft X-ray energies to contain almost 90 % of the $4f^6$ emission. Earlier XPS studies¹ revealed that it is due to the 5^6H and 6^6F multiplets (see upper part of Fig. 1). We shall discuss later why these multiplets are not resolved here, despite the improved resolution with respect to the XPS data. The most interesting feature of Fig. 1 is the dramatic increase of the emission intensity at binding energies around 4.5 eV as a function of photon energy and reaching a maximum at a photon energy 126 eV. We have plotted in Fig. 2A (left scale) the area ratios of the peaks $r_1 = I_2/I_1$. In the region $h\nu < 110$ eV the relative changes of the photo-cross section of the Sm 4f and S 3p levels determine the spectral behaviour of r_1 . Theoretical estimates⁶ indicate a rapid decrease of $\sigma(S, 3p)$ with increasing $h\nu$ up to 40 eV and a broad local maximum at $h\nu = 70$ eV. In addition $\sigma(4f)$ is known to increase monotonically in the region between 15 eV and 70 eV and to remain, apart from resonant effects, rather constant up to 160 eV. At $h\nu_0 = 126.2$ eV r_1 shows a remarkably sharp resonance effect. The resonance has a width of about 3 eV FWHM,

it is asymmetric with a tail at lower photon energies. We interpret this behaviour as a Fano resonance⁸. The interpretation of this resonance effect is facilitated by the data displayed in Fig. 3. Here a constant final state spectrum is presented, measured under identical experimental conditions and on the same SmS surface. The kinetic energy is set at 4 eV while the photon energy is swept through the resonant 4d-4f transition. It is known that CFS spectra at low kinetic energy closely resemble the spectrum of the linear photo-absorption coefficient⁹. The onset of the structure in the CFS spectrum identifies the threshold for the transition $h\nu + 4d^{10}5s^25p^64f^6 \rightarrow 4d^95s^25p^64f^7$. This transition has first been analyzed by Dehmer et al. and by Sugar and it is satisfactorily understood¹⁰. According to the Fano theory⁸ the interaction between Ψ , the quasidecrete level ($4d^95s^25p^64f^7$), with the ionized continuum results in various possible (autoionizing) decay mechanisms:

- (i) $4d^95s^25p^64f^6 + \text{unbound electron}$
- (ii) $4d^{10}5s^25p^64f^5 + \text{unbound electron}$
- (iii) $4d^{10}5s^25p^54f^6 + \text{unbound electron}$
- (iv) $4d^{10}5p^65s^14f^6 + \text{unbound electron.}$

Process (i) has been studied in detail by Dehmer et al.¹⁰. Decay mechanism (ii) is a so called "Super Coster-Kronig" transition and is identified as the origin of the resonant enhancement of the emission intensity near 4.5 eV binding energy (see Fig. 1). It has first been discussed by McGuire in the case of the decay of the 3p hole in transition elements¹¹. Super Coster-Kronig indicates that the principal quantum number of the two electrons and the initial hole involved in the Auger transition are identical. This process is considered to be responsible for the resonance shown by r_1 . The lineshape

of the resonance is given by:

$$\sigma(h\nu) = \sigma_a \frac{(\epsilon + q)^2}{\epsilon^2 + 1} + \sigma_b \quad (1)$$

where $\epsilon = h(\nu - \nu_0)/\Gamma$, and $\Gamma = \hbar \cdot \nu_E^2$ is the half width of the autoionized state. ν_E is the autoionizing (Coulomb) interaction and $q = \langle 4d/r/4f \rangle / \langle \nu_E \langle K/r/\psi \rangle \rangle$. Here $\langle K|$ is the wave function of the outgoing (unbound) electrons and ψ the quasidiscrete level.

By fitting Eq. (1) to the experimental results we find:¹²

$$h\nu_0 = (126.2 \pm 0.2) \text{ eV}, \quad \Gamma = (1.2 \pm 0.1) \text{ eV}, \quad \text{and } q = 4.5.$$

To our knowledge, such a sharp resonant effect has not been observed so far in photoemission from solids. Its origin may rely on the fact that the final state $4f^7$ is a half filled 4f-shell configuration, with first excited state about 3 eV. Detailed calculations for the f^5 and f^6 configurations (Sm^{3+} and Sm^{2+}) are not available.

From Fig. 1 it is also visible, and an analysis confirms it, that the FWHM of the resonance enhanced structure near 4.5 eV reaches a maximum at the resonance frequency $h\nu_0$ pointing towards minimum lifetime of the excited state. But this points needs further investigation. It is tempting to argue that the state ψ can only decay via (ii) by leaving the $4f^5$ shell in the $6p$ state. In fact, a symmetry analysis shows that only multiplets 6F and 6P are allowed as final states participating in the resonance. Preliminary theoretical calculations¹³ indicate the 6P resonant contribution to be about an order of magnitude larger than the 6F . The slight changes in the shape of the structure I_1 with photon energy corroborate this findings, see Fig. 1. The relative insensitivity of I_1 to resonance enhancement justifies our normalization of r_1 . The kinetic energy of unbound electron is in this case expected to be the difference of the photon energy

$h\nu_0$ and the 6P ionization energy.

So far we have not considered channels (iii) and (iv). We identify channel (iii), e.g. $\text{Sm } 5p^6$ emission, as the origin of the additional intensity of the peak labelled I_4 in Fig. 2 B. The photoemission spectrum of the $\text{Sm } 5p^6$ levels itself is not a simple $5p_{3/2}$, $5p_{1/2}$ spin orbit doublet because of the coupling between the $5p^5$ -hole and the open 4f shell. A complete treatment of this spectrum is quite complicated and must include as a final state in the $p^5 f^6$ configuration not only the ground state multiplet 7F_J of the f^6 configuration but also the excited $S = 2$ states which are mixed in by configuration interaction. Detailed calculations that will be presented elsewhere show, in agreement with the experiment, that the major 5p direct emission intensity is contained in the peaks labelled I_3 in Fig. 2 B (see also Fig. 2 C). Peak I_4 in Fig. 2 B is found to show resonance character near the $4d \rightarrow 4f$ threshold. It cannot therefore be solely identified as a direct 5p photoexcitation even if it overlaps in energy in this region ($E_B \sim 23$ eV, see the XPS spectrum in Fig. 2 C). The plot of $r_2 = I_4/I_3$ in Fig. 2 (right scale) confirms the Fano type behaviour. A lineshape analysis using the procedure described above is here not too precise. One obtains roughly: $h\nu_0 = 126.2$, $\Gamma = 1.8$ eV, and $q = -3.2$. We note that Γ and q take different values for the processes (ii) and (iii), which is in itself a further confirmation that the common initial excited state decays via different channels.

Finally we address ourselves to the question of the unresolved 6H and 6F multiplets near the Fermi energy (see Fig. 1, variable photon energy data). We find that the 4f spectrum out of the resonance can be best fitted by using a superposition of two Sm^{3+} -ion final state spectra in agreement with an earlier suggestion³. The two multiplet components are separated by about 0.4 eV,

and have a relative intensity 1:1. We identify them with Sm ions located in and beneath the SmS surface layer, respectively. Their estimated relative intensity is in good agreement with the fraction of the volume defined by the photoelectron escape depth at 120 eV photon energy ($\sim 5 \text{ \AA}$). As one might expect a separation of about 0.4 eV also shows up between the shoulder on the low energy side and the maximum of the $6p$ resonance enhanced structure. Earlier XPS experiments¹⁴ don't seem to indicate this surface induced effect in SmSe and SmTe. However, this is not clear at present since detailed synchrotron radiation studies of these compounds are not yet available.

We would like to thank Prof. E. Bucher for making available SmS single crystals, Dr. C. Kunz and the DESY staff for kindly providing the experimental facilities, G. Kalkoffen for the assistance in the initial set-up of the experiment and Dr. A. Bringer for discussions.

Note added in proof:

When this work was completed we obtained a preprint by Lenth et al. from the DESY group indicating that resonance effects have also been observed in the laser material $\text{Ce P}_{50}\text{O}_{14}$.

References

1. M. Campagna, G.K. Wertheim, and E. Bucher: Structure and Bonding 30, 99 (1976); M. Campagna, G.K. Wertheim and Y. Baer: in "Photoemission in Solids", eds. M. Cardona and L. Ley, Springer Verlag, to be published 1978 and references cited therein.
2. C. Guillot et al., Phys. Rev. Lett. 39, 1632 (1977).
3. G.K. Wertheim, I. Nowik and M. Campagna, Z. Physik B 29, 193 (1978).
4. W. Eberhard, G. Kalkoffen and C. Kunz, Nucl. Instrum. Methods 152, 81 (1978).
5. W. Gudat, S.F. Alvarado and M. Campagna, to be published.
6. D.J. Kennedy and S.T. Manson, Phys. Rev. A 5, 227 (1972).
7. J.L. Freeouf, D.E. Eastman, F. Holtzberg, G.B. Torrance: Phys. Rev. Lett. 33, 161 (1974).
8. U. Fano, Phys. Rev. 124, 1866 (1961).
9. W. Gudat and D.E. Eastman in "Photoemission and the Electronic Properties of Surfaces" eds. B. Feuerbacher, B. Fitton and R.F. Willis, John Wiley and Sons, New York (1978).
10. J.L. Dehmer et al., Phys. Rev. Lett. 26, 1521 (1971), J. Sugar, Phys. Rev. B 5, 1785 (1972).
11. E.I. McGuire, J. Phys. Chem. Solids, 33, 577 (1972).
12. The error on q can be relatively large due to uncertainties in background subtraction. However its sign is well determined.
13. A. Bringer, private communication.
14. M. Campagna, E. Bucher, G.K. Wertheim and L.D. Longinotti, Phys. Rev. Lett. 34, 165 (1974).

Figure Captions

Fig. 1 Photoemission spectrum of the 4f region of SmS using synchrotron radiation in the region near the 4d→4f resonance absorption.

Upper part: X-ray photoemission spectrum using monochromatized Al K_α radiation.

Fig. 2 A: Plot of the ratio $r_1 = I_2/I_1$ and $r_2 = I_4/I_3$ of the area (emission intensity) under the peaks I_2 and I_1 , I_4 and I_3 (see Fig. 2 B)

B: UPS spectrum of SmS at $h\nu = 127$ eV, showing the position of the second resonance around 23-24 eV binding energy.

C: XPS spectrum of isostructural and isoelectronic compound SmTe. This spectrum is shown in order to facilitate identification of Sm 5p direct emission.

Fig. 3 Constant final state spectrum (CFS) of SmS in the region of the resonant absorption 4d-4f. The intensity is normalized to the photoyield of evaporated Au at grazing angles of incidence.

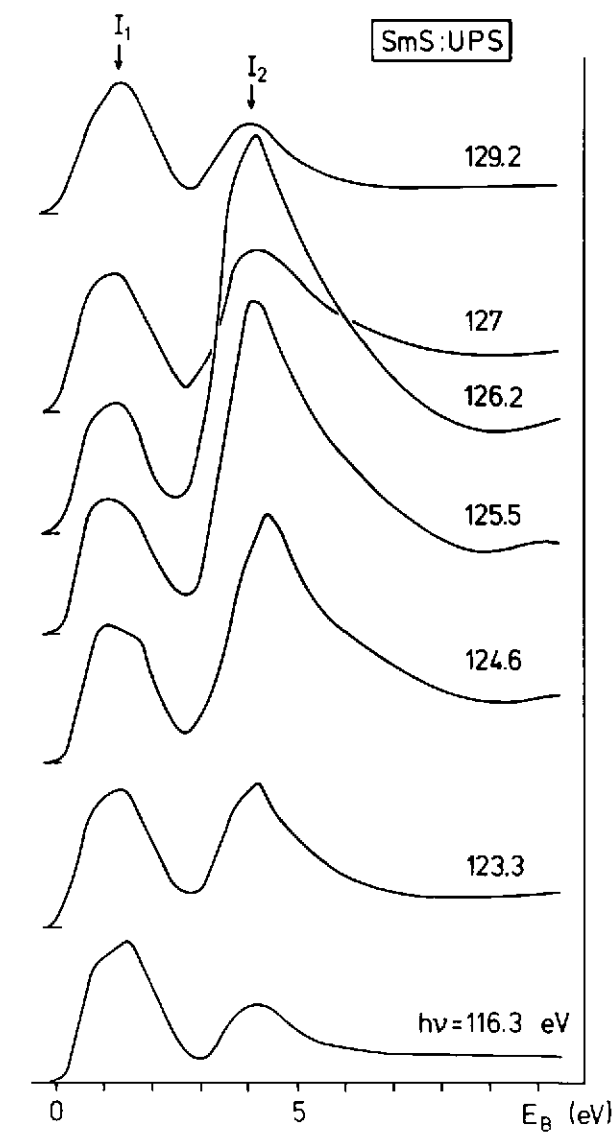
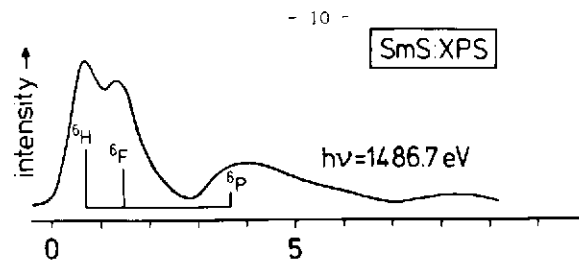


Fig 1

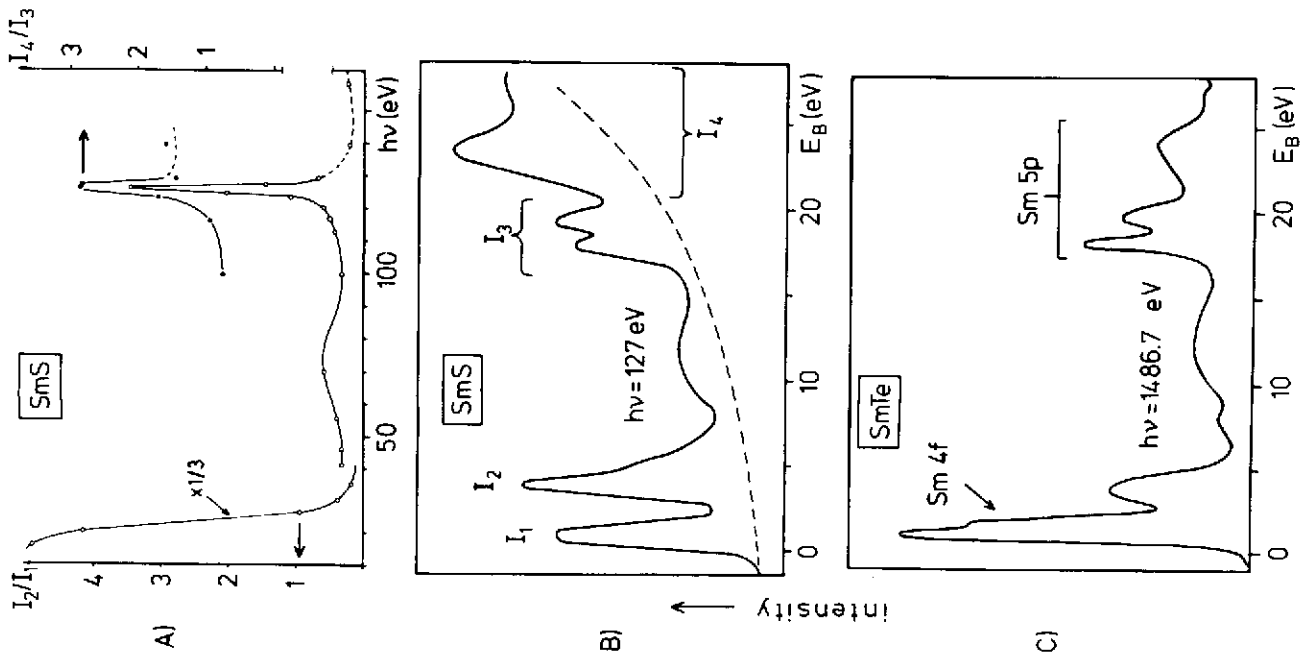


Fig 2

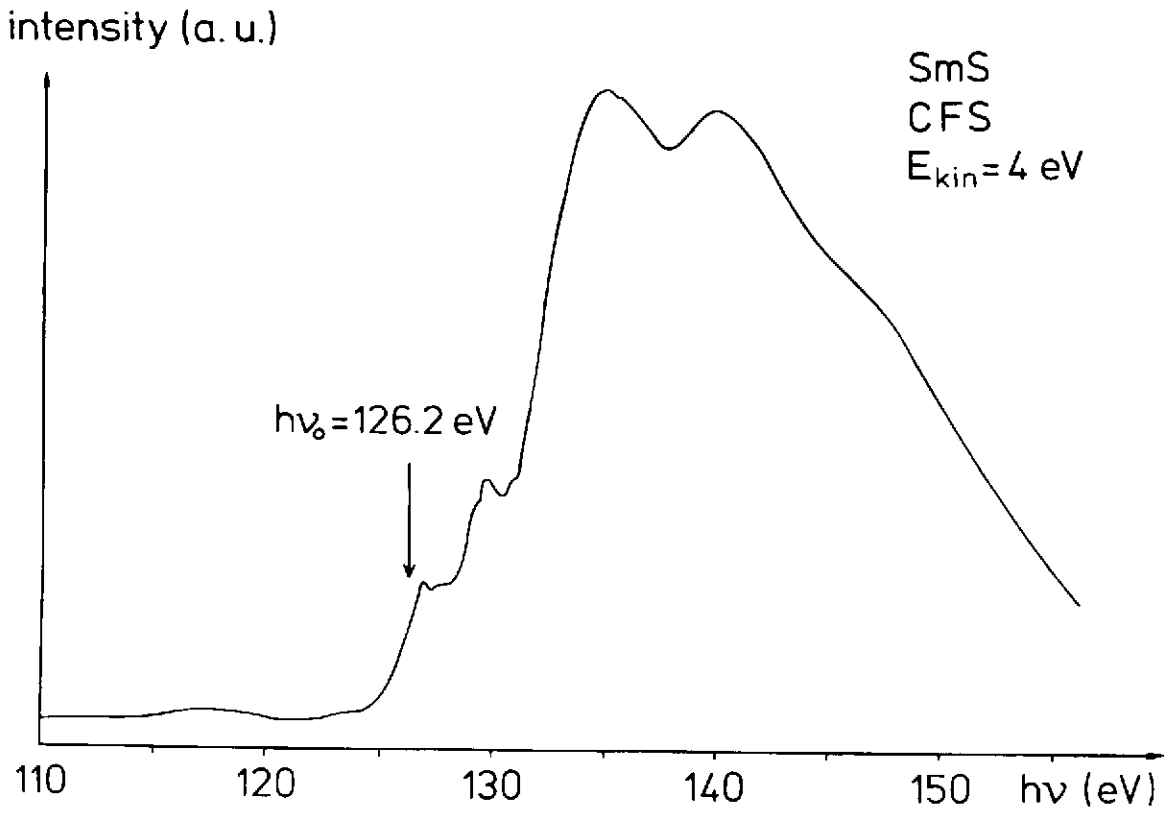


Fig 3